

Classification of Tympanic Membrane Images Based on Deep Learning Model

¹Hamid S. Mahmood, ²Marwan D. Marwan, ^{3*}Mena L. Basheer, ⁴Hafsah R. Amjed, ⁵Marwa Mawfaq Mohamedsheet Al-Hatab

^{1,2,3,4,5}Technical Engineering College, Northern Technical University, Mosul, Iraq

*Corresponding Author's E-mail: menautti45@gmail.com

Abstract - This study investigates the application of Artificial Intelligence (AI) techniques, particularly Convolutional Neural Networks (CNNs), for the diagnosis of tympanic membrane diseases. A dataset comprising 956 tympanic membrane images was collected from various sources, representing conditions such as acute otitis media, chronic otitis media, foreign body presence, tympanosclerosis, and other prevalent disorders affecting the middle ear and tympanic membrane. The images were preprocessed and utilized for training and testing using deep learning methodologies. Several deep learning models were developed and evaluated on the dataset, with systematic optimization of hyperparameters, including the number of filters, filter sizes, and pooling strategies such as Max Pooling and Average Pooling, to enhance classification performance. The proposed models were assessed based on a range of metrics, and the optimal CNN-based model achieved an accuracy of 86.47% in classifying the diseases. The findings of this study underscore the potential of AI-driven solutions to improve medical diagnostics by offering reliable and efficient tools to assist healthcare professionals in the accurate identification of tympanic membrane diseases. Future work is recommended to explore advanced deep learning architectures and expand the dataset to further enhance accuracy and generalizability across diverse medical applications.

Keywords: Classification, Deep Learning, DL, Feature extraction.

I. INTRODUCTION

Humans have a complex organ designed for hearing and balance; the human ear. Anatomically, the ear is divided into three distinct regions: the outer ear, the middle ear, and the inner ear, each of which has its own essential function in the transmission and perception of sound. The outer ear consists of the auricle and external auditory canal, which funnels sound waves toward the tympanic membrane (eardrum). The middle

ear contains the ossicles (malleus, incus, and stapes), which amplify sound vibrations, and the inner ear contains the cochlea and vestibular system for auditory processing and balance regulation Figure 1[1].

Any structural abnormalities and/or infections in these components can lead to hearing loss or other medical conditions [2]. Precise diagnosis of middle ear ailments, especially those involving the tympanic membrane, is critical for appropriate management. Common diseases such as otitis media, tympanic membrane perforation, and cholesteatoma should be accurately diagnosed by otoscopic examination [3]. However, manual diagnosis relies on clinician expertise, introducing the potential for interobserver variability and misclassification [4]. In order to address these issues, many artificial intelligences (AI) based approaches have been investigated to improve accuracy and efficiency when classifying tympanic membrane (TM) images [5].

Medical imaging analysis is a major application of deep learning, a subset of AI, with CNNs (Convolutional Neural Networks) achieving notable excellence in this field. Convolutional Neural Networks (CNNs) automatically extract hierarchical features from images, making them well-suited for effective classification of pathological and normal TM conditions [6]. Inception V3 is one of the most popular CNN architectures because of its efficiently-designed depth and factorized convolutions, which provide better feature extraction but lower computation complexity [7]. Its classification became an important proposition since CNNs demonstrated successful classification results through otoscopic images [8].

This study intends to build a classification model based on AI by utilizing the Inception V3 network capable of recognizing the TM conditions based on otoscopic images. The diagnostic aims to increase diagnostic accuracy and support healthcare professionals in the early detection of diseases, ultimately enhancing patient outcomes [9] [10] [11-14].

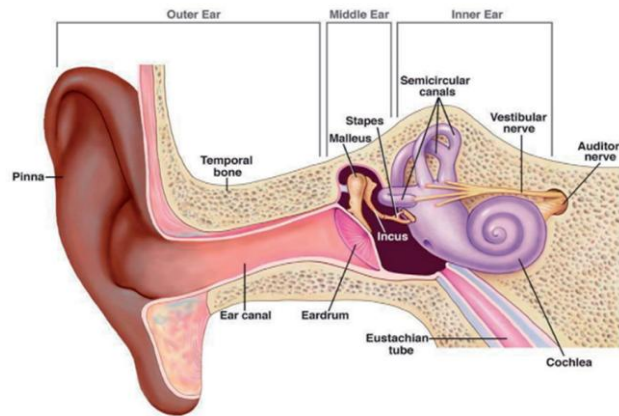


Figure 1: Structure of the mammalian ear

II. MATERIALS AND METHODS

In this study, a new scheme is presented to classify activities related to the tympanic membrane. Deep learning (DL) networks are designed, combined, and implemented to achieve high classification accuracy. This work consists of multiple logical stages. First, images of the tympanic membrane are collected, documenting different patterns based on anatomical and physiological characteristics. Additionally, the images are divided into two sets: one for the training phase and another for the testing phase. Customized DL models are designed to process and analyze tympanic membrane images. These models are trained using the training dataset and tested with the testing dataset. Moreover, DL parameters, such as convolution and pooling layers, are evaluated to achieve the highest accuracy. Finally, the outputs of the proposed models are fused to enhance the reliability of classification decisions, taking into account the various characteristics of the tympanic membrane. Fig 2 illustrates the proposed new scheme and outlines the required processing stages in this study.

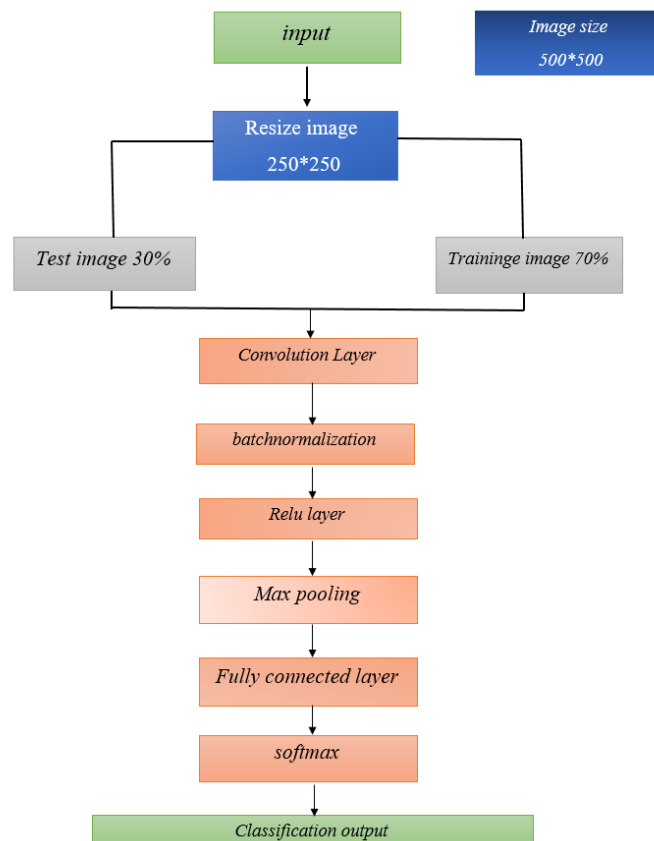


Figure 2: The proposed efficient model to classify Tympanic membrane images

2.1 Data set

The dataset consists 956 images divided into the following categories: Normal Tympanic Membrane images Acute Otitis Media(AOM):images Chronic Otitis Media images Ear Ventilation images Earwax images Foreign Body images Otitis Externa images Pseudo Membrane images Tympanosclerosis images The images were captured with standard dimensions of 500×500×3 pixels in joint photographic group (JPG) format. This dataset provides a comprehensive foundation for analyzing and detecting tympanic membrane disorders [15].

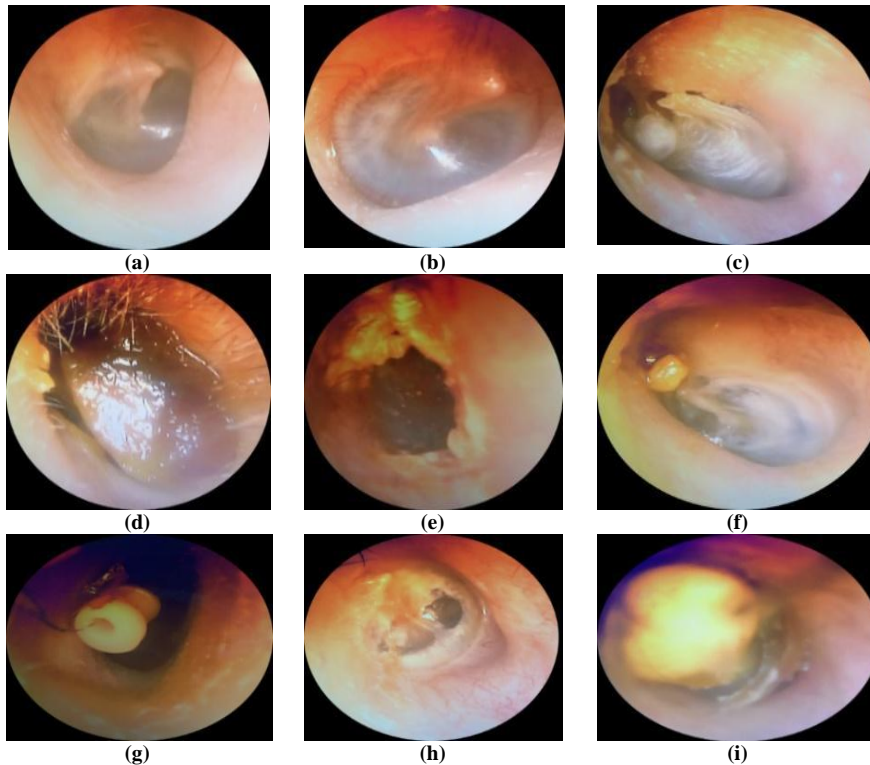


Figure 3: Normal and abnormal Tympanic Membrane images (a) normal, (b) AOM, (c) Chronic, (d) Earwax, (e) Otitis externa, (f) Tympanosclerosis, (g) Ear ventilation tube, (h) Pseudo-membranes and (i) Foreign

III. CNN

First of all, people have benefited from the Artificial Intelligence (AI) in various fields such as pattern recognitions, musical recommender systems, natural language processing, games, Google maps and many more applications. Many algorithms are suggested to build intelligent programs and systems which can creatively solve problems. Machine learning (ML) is a subset of the AI, it provides algorithms that have the ability to automatically learn and improve the intelligent applications or systems [16]. DL is a subset of the ML, it is a hot and advanced topic of the ANN [17]. It can analyze different and large amounts of data. Fig 4 shows an illustration of the relationships between the AI, ML, and DL.

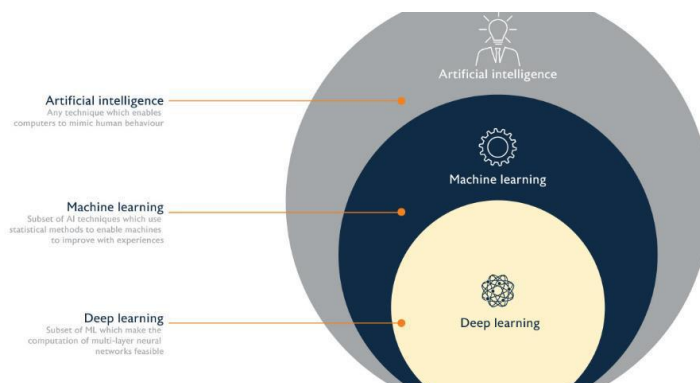


Figure 4: The relationships between the AI, ML and DL

In recent years, ANNs have yielded limitations when they come to process a large-scale of different dataset types such as images or videos. Therefore, the CNN is developed and it has become a solution to many computer vision problems in the ML field [16]. It is considered as one of many DL networks. Its algorithms can offer a clear understanding of image analysis by providing exemplary implementation to image feature extraction, classification and retrieval related tasks [17] [18]. It is even successfully applied to natural language processing, recommender systems and even industrial. One of the main CNN advantages compared to its predecessors is that it can automatically detect image features (feature extraction) without a human supervision. Moreover, the CNN is computationally efficient. This makes it universally attractive. In 1988s, Le Cun proposed the CNN [19]. However, it was dormant until the mid of 2000s, when computers are developed and can analyze a big number of data. This development led to facilitate employing the CNN and improving its algorithms. It was a big breakthrough neural network. This technique occupies prominent position in computer vision. It has been utilized in various medical applications such as neuronal membrane segmentation for electron microscopy images [20], carotid intima-media thickness measurement for ultrasound images [21], detection of pulmonary embolism [22], detection breast cancer [23] and brain tumor segmentation for MRI scans [24]. It has also successfully exploited for other applications as English handwritten recognition [25] and image reconstruction [26]. Furthermore, some companies have developed active research groups for exploring new CNN architectures such as Google, Microsoft, Network Edge Compute (NEC) and Facebook [27]. CNN uses the convolution in at least one layer [28]. Its architecture is typically comprised of multiple layers. Basically, it contains the input layer, multiple hidden layers and output or classification layer. The multiple hidden layers typically consist of a series of layers, each for a specific function and task such as convolution, Rectified Linear Unit (ReLU), pooling, Fully Connected (FC) and softmax layers. They are stacked to form a deep model. An image is directly input to the network, then, it will be analyzed for feature extractions by passing through a number of convolution, ReLU and pooling layers. Subsequently, the resulted outcomes will be classified in the classification part by passing through the FC, softmax and classification layers. So, the CNN has two fundamental parts: feature extraction and classification, where each one of them has multiple layers. A general architecture of the CNN for the image classification task can be seen in Fig. 5. Technically, the CNN model requires two phases: training and testing, just as other ML techniques.

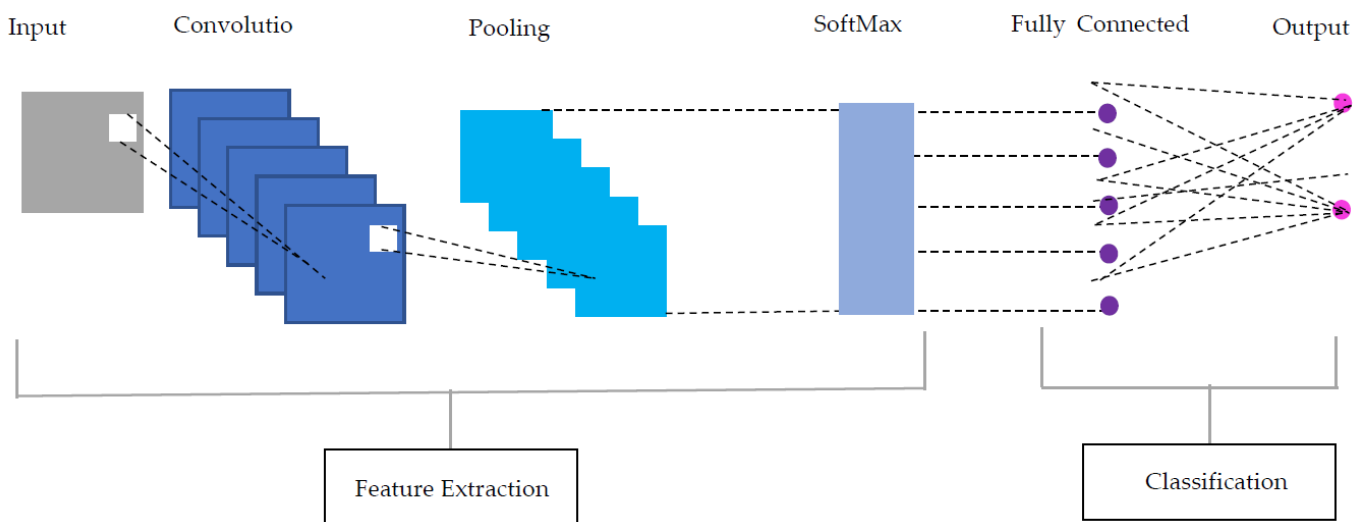


Figure 5: A general CNN architecture for the image classification task

3.1 Input Layer

The input layer handles images by taking in pixel values according to the resolution and dimensions of the image. In this research, JPG color images with dimensions (width × height × 3) are utilized. The "3" represents the RGB color channels—Red, Green, and Blue—that make up the complete color image.[29]

3.2 Convolution Layer

The convolution layer utilizes various kernels (filters) on the input image channels, generating feature maps that emphasize particular patterns. Each kernel functions as a group of adjustable weights, convolving across small sections of the input. This process retrieves spatial characteristics crucial for more in-depth examination.[30][31][32]

$$F_{u,v,c}^l = U_c^l + \sum_{i=-H_h^l}^{H_h^l} \sum_{j=-H_w^l}^{H_w^l} \sum_{c^{l-1}=1}^{c^{l-1}} W_{i+H_h^l,j,H_w^l,c}^{c^{l-1}} F_{u+i,v+j,c^{l-1}}^{l-1} \quad (1)$$

Where: $F_{u,v,c}^l$ is an output of the convolution layer, (u,v) is a pixel coordinate, c is the channel number, l is the current layer, U_c^l is the channel bias, H_h^l and H_w^l are respectively the height and width of the convolution layer kernel, $l - 1$ is the previous layer, and $W_{i,j,c^{l-1}}^{c^{l-1}}$ is the kernel weights.

3.3 ReLU Layer

The ReLU layer adds non-linearity by transmitting only positive values while converting negative ones to zero. It simulates neuron activation, enabling the model to understand intricate patterns. This renders it crucial in CNNs for effective feature extraction.[31]

$$R_{u,v,c}^l = \text{MAX}(0, F_{u,v,c}^l) \quad (2)$$

Where: $R_{u,v,c}^l$ is the output of ReLU, MAX is the maximum operation and $F_{u,v,c}^l$ is an input positive value to the ReLU activation function [33].

3.4 Pooling Layer

The pooling layer carries out down-sampling to decrease the spatial dimensions of feature maps while maintaining depth. Used post-ReLU, it reduces pixel numbers and aids in avoiding overfitting, enhancing the model's efficiency and generalization.[34][35]

3.5 Softmax Layer

The softmax layer transforms the final outputs into probability distributions across all potential classes. Situated prior to the classification layer, it assists in choosing the most probable class but may become costly in terms of computation when dealing with numerous classes.[31]

$$y_r = \frac{\exp(P_r)}{\sum_{s=1}^{n^{l-1}} \exp(P_s)} \quad (3)$$

Where: y_r is an output of the softmax layer.

3.6 Fully Connected Layer

The fully connected (FC) layer connects every neuron from the preceding layer to each neuron in its own layer. It connects the feature extraction and classification sections of the model, allowing for final decision-making based on the features extracted.[36]

$$P_r = \sum_{a=1}^{n_1^{l-1}} \sum_{b=1}^{n_2^{l-1}} \sum_{c=1}^{n_3^{l-1}} U_{a,b,c,r}^l (T_s)_{a,b} \quad \forall 1 \leq r \leq n^l \quad (4)$$

Where: P_r is an output of the FC layer, n_1^{l-1} is the previous pooling channel width, n_2^{l-1} is the previous pooling channel height, n_3^{l-1} is the number of previous pooling channels, $(T_s)_{a,b}$ is a pooling layer output, $U_{a,b,c,r}^l$ is a weight between the pooling and FC layers, and n^l is the required number of nodes in the current FC layer.

3.7 Classification Layer

The classification layer is the last decision-making layer that assigns the input to the most likely category. It adheres to the "winner-takes-all" principle, choosing the class that has the highest predicted likelihood.[30]

$$D_r = \begin{cases} 1 & \text{if } y_r = \max \\ 0 & \text{otherwise} \end{cases} \quad (5)$$

Where: D_r is an output decision of the classification layer and max represents the extracted maximum y_r value.

IV. RESULT AND DISCUSSION

In this ponder, it has been presented information set in it has been utilized a Lenovo LOQ Gaming portable workstation with an Intel Center i7-13620H processor, 2.40GHz, 16GB Slam, NVIDIA GeForce RTX 4060 portable workstation GPU, and 8GB GPU memory and after that applied it into MATLAP and include *feature extractions, Convolution Layer, batchnormalization, Relu layer, Max pooling, Fully connected layer, softmax, Classification output*. It has been isolated information preparing training 70% and test 30%.

Table 1: Classification results of deep learning model

case	conv				ty	pooling			accuracy
	filter size	no of filter	stride	padding		size	stride	padding	
1	3*3	2	1	1	max	3x3	1	1	79.2271
	5*5	2	1	1	max	3x3	1	1	74.8792
	7*7	2	1	1	max	3x3	1	1	79.7101
	9*9	2	1	1	max	3x3	1	1	81.1594
	11*11	2	1	1	max	3x3	1	1	77.2947
	13*13	2	1	1	max	3x3	1	1	82.1256
	15*15	2	1	1	max	3x3	1	1	79.2271
2	13x13	2	1	1	max	3x3	1	1	82.1256
	13x13	4	1	1	max	3x3	1	1	71.0145
	13x13	6	1	1	max	3x3	1	1	77.7778
	13x13	8	1	1	max	3x3	1	1	75.8454
	13x13	10	1	1	max	3x3	1	1	77.2947
	13x13	12	1	1	max	3x3	1	1	78.744
	13x13	14	1	1	max	3x3	1	1	74.3961
3	13x13	2	1	1	max	3x3	1	1	82.1256
	13x13	2	2	1	max	3x3	1	1	84.058
	13x13	2	3	1	max	3x3	1	1	80.6763
	13x13	2	4	1	max	3x3	1	1	76.8116
	13x13	2	5	1	max	3x3	1	1	72.9469
	13x13	2	6	1	max	3x3	1	1	77.7778
	13x13	2	7	1	max	3x3	1	1	74.3961
4	13x13	2	2	0	max	3x3	1	1	79.7101
	13x13	2	2	1	max	3x3	1	1	84.058
	13x13	2	2	2	max	3x3	1	1	83.5749
	13x13	2	2	3	max	3x3	1	1	80.6763
	13x13	2	2	4	max	3x3	1	1	81.6425
	13x13	2	2	5	max	3x3	1	1	75.3623
	13x13	2	2	6	max	3x3	1	1	82.1256
5	13x13	2	2	1	max	3x3	1	1	84.058
	13x13	2	2	1	avg	3x3	1	1	78.2609
	13x13	2	2	1	max	3x3	1	1	84
	13x13	2	2	1	max	5x5	1	1	86.4734
6	13x13	2	2	1	max	7x7	1	1	84.058
	13x13	2	2	1	max	9x9	1	1	85.9903
	13x13	2	2	1	max	11x11	1	1	81.1594
	13x13	2	2	1	max	13x13	1	1	84.5411
	13x13	2	2	1	max	15x15	1	1	85.9903
	13x13	2	2	1	max	5x5	1	1	86.4734
7	13x13	2	2	1	max	5x5	2	1	84.058
	13x13	2	2	1	max	5x5	3	1	78.2609
	13x13	2	2	1	max	5x5	4	1	79.7101
	13x13	2	2	1	max	5x5	5	1	74.3961
	13x13	2	2	1	max	5x5	6	1	77.7778
	13x13	2	2	1	max	5x5	7	1	76.3285
	13x13	2	2	1	max	5x5	1	0	85.5072
8	13x13	2	2	1	max	5x5	1	1	86.4734
	13x13	2	2	1	max	5x5	1	2	83.0918
	13x13	2	2	1	max	5x5	1	3	81.1594
	13x13	2	2	1	max	5x5	1	4	82.6087
	13x13	2	2	1	max	5x5	1	5	NON
	13x13	2	2	1	max	5x5	1	6	NON

After conducting several experiments on 5 cases, data was trained using a CNN network. The outer folder, which contained only 3 images, was removed as it negatively affected the network's accuracy due to the insufficient number of images. Additionally, the cases AOM, chronic, and Otitis externa were removed because they refer to the same disease, inflammation, differing only in the severity of inflammation. The degrees of inflammation include chronic and acute inflammation. The tympanosclerosis file was considered sufficient as it is similar to the aforementioned cases. Two other files were also removed to enhance accuracy. The dataset was divided into 8 cases, and the parameters were adjusted and distributed over seven stages for each case, with only one parameter changed in each stage, as shown in Table 3. The filter size in the convolutional layers was changed from 3x3 to 15x15, achieving the highest accuracy at 13x13 with an accuracrate of 82.1256%.The number of filters in the convolutional layers was changed from 2 to 14 while keeping the filter size at 13x13. The highest accuracy of 82.1256% was achieved using only 2 filters. The stride value in the convolutional layers was changed from 1 to 7 while keeping the number of filters and filter size constant, achieving the highest accuracy of 84.058% at a stride of 2.The padding values in the convolutional layers were changed from 0 to 6 while keeping the other parameters constant, achieving the highest accuracy of 84.058% at a padding of 1.The comparison between max pooling and average pooling showed that max pooling was better, achieving the

highest accuracy of 84.058%. The max pooling size was changed from 3×3 to 15×15, achieving the highest accuracy of 86.4734% at a size of 5×5. The stride value in max pooling was changed from 1 to 7, achieving the highest accuracy of 86.4734% at a stride of 1. The padding values in max pooling were changed from 0 to 6, achieving the highest accuracy non.

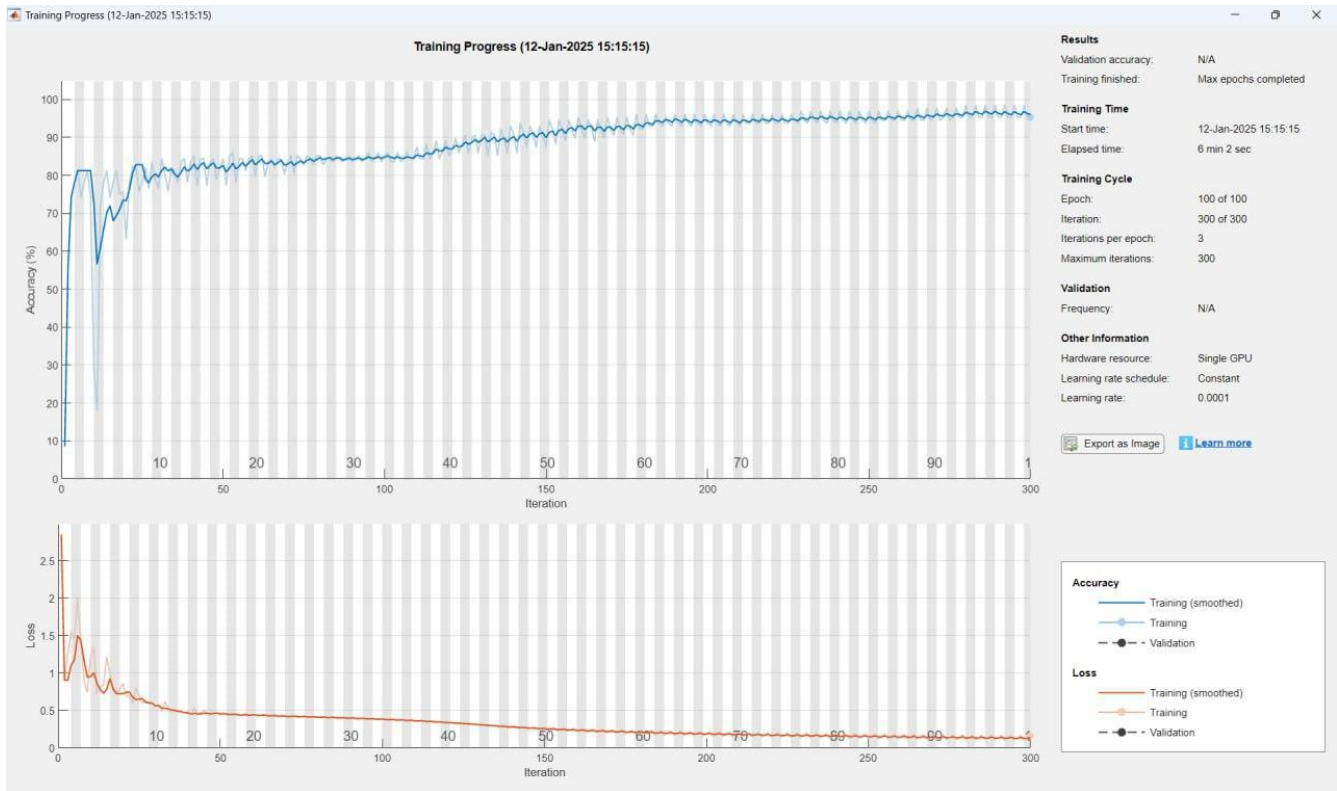


Figure 6: Training process (Accuracy and loss) for dataset

In this figure show relationship between accuracy and Iteration, loss and Iteration, number of epoch, Iteration per epoch, maximum Iteration, validation accuracy. The loss could significantly be reduced and the accuracy could dramatically be increased to the highest value.

V. CONCLUSION

In this paper, accurate diagnosis of tympanic membrane diseases is very important. In this study, we applied the feature extraction layers, and the model was more effective, and we obtained the highest accuracy of 86.4734%.

REFERENCES

- [1] H. W. Gelfand, Essentials of Audiology, 4th ed. New York, NY, USA: Thieme, 2016.
- [2] M. R. Clark and A. P. Smith, "Hearing loss and middle ear pathologies: A clinical overview," *Otolaryngology Clinics*, vol. 52, no. 1, pp. 23–38, 2020.
- [3] L. K. Hunter et al., "Otitis media: Diagnosis, management, and complications," *Pediatrics Review*, vol. 41, no. 5, pp. 220–235, 2019.
- [4] S. S. Mehta et al., "Variability in diagnosing tympanic membrane abnormalities: A systematic review," *Journal of Otolaryngology Research*, vol. 15, no. 2, pp. 101–115, 2021.
- [5] J. C. Wang et al., "Artificial intelligence in otoscopic image analysis: A review," *IEEE Transactions on Biomedical Engineering*, vol. 69, no. 4, pp. 1172–1185, 2022.
- [6] A. Krizhevsky, I. Sutskever, and G. Hinton, "ImageNet classification with deep convolutional neural networks," in *Advances in Neural Information Processing Systems (NIPS)*, vol. 25, pp. 1097–1105, 2012.
- [7] C. Szegedy et al., "Rethinking the Inception architecture for computer vision," in *Proc. IEEE Conf. Comput. Vis. Pattern Recognit. (CVPR)*, Las Vegas, NV, USA, 2016, pp. 2818–2826.
- [8] J. D. Livingstone et al., "Deep learning-based classification of otoscopic images for eardrum abnormalities," *IEEE Access*, vol. 8, pp. 182332–182341, 2020.
- [9] M. Mohammad, W. R. Fathel, H. D. Ali, and M. M. Al-Hatab, "Enhanced non-invasive blood glucose monitoring system employing wearable optical

- technology," *Fusion: Practice and Applications (FPA)*, vol. 19, no. 1, Jan. 2025. DOI: 10.54216/FPA.190101.
- [10] K. H. J. Al-Bahar, "Integrated artificial intelligence approach for diabetic foot ulcer assessment: A comprehensive solution for precision diagnosis and patient care," *Adv. Knowl.-Based Syst. Data Sci. Cybersecurity Res.*, vol. 1, no. 1, p. 4, 2024.
- [11] M. A. Malla et al., "Adopting machine learning to automatically identify a suitable surgery type for refractive error patients," *Jurnal Kejuruteraan*, vol. 36, no. 4, pp. 1749–1757, 2024.
- [12] M. M. M. Al-Hatab, A. S. I. Al-Obaidi, and M. A. Al-Hashim, "Exploring CIE Lab color characteristics for skin lesion images detection: A novel image analysis methodology incorporating color-based segmentation and luminosity analysis," *Fusion: Practice and Applications*, vol. 15, no. 1, pp. 88–97, 2024.
- [13] R. R. O. Al-Nima, M. M. M. Al-Hatab, and M. A. Qasim, "An artificial intelligence approach for verifying persons by employing the deoxyribonucleic acid (DNA) nucleotides," *J. Electr. Comput. Eng.*, vol. 2023, no. 1, Art. no. 6678837, 2023.
- [14] W. R. Fathel, M. M. Al-Hatab, and M. A. Qasim, "Classification of ECG signals based on k-nearest neighbors (k-NN) algorithm," *Eurasian J. Eng. Technol.*, vol. 16, Mar. 2023, ISSN: 2795-7640.
- [15] E. Basaran, "Tympanic membrane / eardrum dataset / otitis media," Kaggle, 2024. [Online]. Available: <https://www.kaggle.com/datasets/erdalbasaran/eardrum-dataset-otitis-media>. [Accessed: Feb. 21, 2025].
- [16] M. L. Kolhe, M. C. Trivedi, S. Tiwari and V. K. Singh, "Advances in Data and Information Sciences.," *Proceedings of ICDIS*, vol. 1, 2017.
- [17] Z. B. Tekulu and S. Wenxuan, "Schizophrenia Disease Classification with Deep learning and Convolutional Neural Network Architectures using TensorFlow.," 2019.
- [18] K. Yasaka, H. Akai, O. Abe and S. Kiryu, "Deep Learning with Convolutional Neural Network for Differentiation of Liver Masses at Dynamic Contrast-Enhanced CT: A Preliminary Study.," *Radiology*, vol. 3, no. 286, 2018.
- [19] Y. Lecun., "Generalization and Network Design Strategies.," *Connectionism in perspective*, vol. 19, no. 143, 1989.
- [20] S. Sudha, K. B. Jayanthi, C. Rajasekaran, N. Madian and T. Sunder, "Convolutional neural network for segmentation and measurement of intima media thickness.," *Journal of medical systems*, vol. 8, no. 42, 2018.
- [21] S. Savaş, N. Topaloğlu, Ö. Kazıcı and P. N. Koşar, , "Classification of Carotid Artery Intima Media Thickness Ultrasound Images with Deep Learning.," *Journal of medical systems*, vol. 8, no. 43, 2019.
- [22] C. Zhou, H. P. Chan, S. Patel, P. N. Cascade, B. Sahiner, L. M. Hadjiiski and E. A. Kazerooni, "Preliminary Investigation of Computer-aided Detection of Pulmonary Embolism in Three Dimensional Computed Tomography Pulmonary Angiography Images.," *Academic radiology*, vol. 6, no. 12, 2005.
- [23] T. Mahmood, M. Arsalan, M. Owais, M. B.Lee and K. R. Park, "Artificial Intelligence-Based Mitosis Detection in Breast Cancer Histopathology Images Using Faster R-CNN and Deep CNNs.," *Journal of Clinical Medicine*, vol. 3, no. 9, 2020.
- [24] S. Iqbal, M. U. Ghani, T. Saba, and A. Rehman, "Brain Tumor Segmentation in Multi-spectral MRI Using Cconvolutional Neural Networks (CNN). ," *Microscopy research and technique*, vol. 4, no. 81, 2018.
- [25] A.Yuan, G. Bai, L. Jiao and Y. Liu, "Offline Handwritten English Character Recognition Based on Convolutional Neural Network. In: 2012 10th IAPR International Workshop on Document Analysis Systems", *IEEE*, 2012.
- [26] A.Krizhevsky, I. Sutskever and G. E. Hinton, "Imagenet Classification with Deep Convolutional Neural Networks", In: *Advances in neural information processing systems*. 2012.
- [27] J. Yangqing, E. Shelhamer, J. Donahue, S. Karayev, J. Long, R. Girshick , T. Darrell, "Caffe: Convolutional Architecture for Fast Feature Embedding", In: *Proceedings of the 22nd ACM international conference on Multimedia.*, 2014.
- [28] K. Christoff, G. Glover, R. Charms, "Learned Regulation of Spatially Localized Brain Activation Using Real-time fMRI," *Neuroimage*, vol. 21, no. 436, 2004.
- [29] P. Khaire, P. Kumar and J. Imran, "Combining CNN streams of RGB-D and Skeletal Data for Human Activity Recognition", *Pattern Recognition Letters*, 2018.
- [30] R. R. O. Al-Nima, "Signal Processing and Machine Learning Techniques for Human Verification Based on Finger Textures.," *Newcastle University.*, 2017.
- [31] R. R. Omar, T. Han, S. A. Al-Sumaidae and T. Chen, "Deep Finger Texture Learning for Verifying People.," *IET Biometrics*, vol. 1, no. 8, 2018.
- [32] C. L. Huang and C. Y. Tsai, "A hybrid SOFM-SVR with a Filter-based Feature Selection for Stock Market Forecasting", *Expert Systems with Applications*, vol. 2, no. 36, 2009.

- [33] J. Brownlee, "A Gentle Introduction to Padding and Stride for Convolutional Neural Networks". 2019.
- [34] A.Khan, A. Sohail, U. Zahoor and A. S. Qureshi, "A Survey of the Recent Architectures of Deep Convolutional Neural Networks", *Artificial Intelligence Review*, 2019.
- [35] M. Ahmed, F. Girshick, R. Zitnick, L. Batra, D. Cogswell, "Reducing Overfitting in Deep Networks by Decorrelating Representations", *arXiv preprint arXiv:1511.06068*, 2015.
- [36] W. Ma and J. Lu, "An Equivalence of Fully Connected Layer and Convolutional Layer", *arXiv preprint arXiv:1712.01252*, 2017.

Citation of this Article:

Hamid S. Mahmood, Marwan D. Marwan, Mena L. Basheer, Hafsah R. Amjed, & Marwa Mawfaq Mohamedsheet Al-Hatab. (2025). Classification of Tympanic Membrane Images Based on Deep Learning Model. *International Research Journal of Innovations in Engineering and Technology - IRJIET*, 9(5), 42-50. Article DOI <https://doi.org/10.47001/IRJIET/2025.905005>
